Separating Internal Waves and Vortical Motions: Analysis of LatMix χ-EM-APEX Float Measurements

Ren-Chieh Lien
Applied Physics Laboratory
University of Washington
1013 NE 40th Street
Seattle, Washington 98105
Phone: (206) 685-1079 fax: (206) 543-6785 email: lien@apl.washington.edu

Thomas B. Sanford
Applied Physics Laboratory and School of Oceanography
University of Washington
1013 NE 40th Street
Seattle, Washington 98105
Phone: (206) 543-1365 fax: (206) 543-6785 email: sanford@apl.washington.edu

Award Number: N00014-15-1-2184

LONG-TERM GOALS

Our long-term scientific goals are to understand the dynamics and identify mechanisms of small-scale processes—i.e., internal tides, inertial waves, nonlinear internal waves, vortical modes, and turbulence mixing—in the ocean and thereby help develop improved parameterizations of mixing for ocean models. Mixing within the stratified ocean is a particular focus as the complex interplay of internal waves from a variety of sources and turbulence makes this a current locus of uncertainty. Our focus is on observing processes that lead to lateral mixing of water properties. The exploitation of autonomous platforms is a long-term goal.

OBJECTIVES

Our primary scientific objective is to use an innovative swarm of autonomous profilers to improve our understanding and parameterization schemes of small- to submeso-scale oceanic processes. Dispersion due to lateral processes with vertical and horizontal shears could enhance turbulent mixing. Both internal waves and vortical motions exist at vertical scales smaller than order of 10 m and horizontal scales smaller than a few km. They have distinct kinematics and dynamics. Internal waves propagate and may carry energy to remote regions before they break and dissipate via turbulent processes, whereas vortical motions do not propagate and are often long lived. Separation of these two motions is necessary to improve parameterization schemes.

APPROACH

Our approach is to study the internal wave background, shear vector, vorticity vector, and turbulent mixing using measurements taken by a "swarm" of EM-APEX profiling floats in the Sargasso Sea.

EM-APEX floats profile simultaneously through the surface mixed layer and upper seasonal pycnocline every hour (Fig. 1). These 3-D observations of turbulence, instability, and small-scale processes are vital to understanding the dynamics of the coupling between the diapycnal mixing and oceanic lateral processes. Our primary purposes are to separate small-scale vortical motions and internal waves and quantify their effects on horizontal dispersion and diapycnal mixing.

WORK COMPLETED

- Participated in LatMix meeting at Stanford in January 2013
- Quality control and submission of data to LatMix server
- Adjusted EM-APEX relative velocity to absolute velocity using GPS fixes for every surfacing of the floats and compared the processed absolute velocities to nearby ADCP shipboard data for quality assurance
- Computed quasi-Lagrangian quantities, such as relative vorticity, horizontal divergence, vortex stretching and potential vorticity, projected onto isopycnal surfaces for three deployments
- Developed algorithm using Kelvin's circulation and a linear regression to find horizontal gradients in higher order computed quantities, specifically PV
- Computed vortex stretching to compare with relative vorticity
- Tested consistency relations for linear internal waves: PE/KHE and CCW/CW spectra
- Presented results at the ONR Peer Review in Chicago in September 2013
- Presented results at the Ocean Sciences Meeting in Honolulu in February 2014
- Reprocessed and improved quality of EM-APEX velocity observations in 2015
- Quantified velocity uncertainty of EM-APEX velocity observations in 2015
- Continued analysis in different energetic regimes in 2015

Experiment Recap:

Our cruise on the R/V *Endeavor*, 1–21 June 2011, involved three EM-APEX deployments imbedded within the three-ship LatMix experiment. Two varieties of floats were used: a) 11 standard floats that measure U, V, T, S, and P and b) 10 that also measured χ, the thermal variance diffusion rate. The floats were programmed to rise to the surface at the same time. In addition to Slocum gliders and Lagrangian floats, three-ship ADCP, S, T, P, and dye concentration surveys were conducted for each setting. Operations and observations included:

i) Large-scale (15 x 15 km radiator pattern), 18-hour background field on the R/V *Oceanus*

ii) 10-km, 4-hour butterfly pattern following dye patches on R/V *Endeavor*

iii) Dye following to track the advection and mixing of the dye patches on R/V *Cape Hatteras*

The first region was dubbed "Big Nothing" based on minimal upper ocean property gradients. Twenty-one EM-APEX floats were deployed in three concentric circles of radii 0.5, 1 and 2 km late on 3 June and evolved until 10 June, with some floats rearranged in the middle of the time series to reduce

ellipticity of the arrangement (Fig. 2). On 7 June, the array was carried into a more dynamic region with increasing southwest velocity, which caused the array to reshape into an ellipse with a NW–SE dominant axis.

The second region (30 km north of setting 1) was surveyed and chosen based on its large property gradients. On 13 June, 19 floats were deployed in the same concentric circle orientation near the dye release. The initial location was in a stagnation point, where the floats remained for about 24 hours before being transported to the northeast, with strong south-east/north-west gradients. The other assets were moved northward immediately, causing an increasing separation between the EM-APEX float array and most other instruments. The strong strain necessitated recovery and repositioning of some floats to maintain a circular form. Despite this, for most of this experiment and setting 3, the float orientation was elongated in the NE–SW direction, with aspect ratio near 5 to 1. The floats were recovered on 17 June.

The third setting was slightly downstream of the evolving dye injections in anticipation of being overtaken and measuring similar ocean properties from 17 June through 20 June. Again, the high strain caused an elongation of the floats, though adding two floats halfway through this deployment helped maintain circularity of the array.

Summary of observations:

- Innovative new use of multiple, autonomous vertical profilers to collect simultaneous profiles of U, V, T, S and χ in the upper ocean on horizontal scales of 10 m to 10 km
- Obstacle avoidance system developed and installed on each R/V's bridge informed watch of the locations of various platforms on the surface
- 21 EM-APEX floats, including 10 with χ sensors, deployed in 3 settings with a single profiler lost
- 9274 vertical profiles obtained from surface to 100 m or deeper, 99.9% had CTD profiles, 90.1% yielded velocity profiles
- 2056 profiles had fast temperature gradient observations for χ (and ε), and 1792 or 87.7% yielded good data

RESULTS

Quality assessment of EM-APEX velocity measurements

To ensure quality of processing and reliability of measurements, several steps have been taken. All velocity measurements were removed if the Verr (i.e., velocity uncertainty) of the fit to the voltage was above 1 cm s^{-1}, or the vertical profiling speed of the float was less than 0.05 m s^{-1}, or the rotation period of the float was greater than 25 s. Depth-averaged, array-averaged estimated velocities from surface GPS position fixes were computed to adjust the measured relative velocity to absolute velocity profiles. Consistency between simultaneous, nearby floats was examined by plotting the relationship between the square (kinetic energy) of the depth-averaged velocity differences and the float separation distance. This gives an estimate of the inherent instrument noise of about 1–2 cm s^{-1}.

Review: Vortical motion and internal wave theory

The primary scientific goal of this project is to separate internal waves and vortical motions. These two processes coexist at small spatial scales (Müller 1984). However, they have distinct kinematic and dynamic properties. Vortical motions carry Ertel's potential vorticity and internal waves do not. Ertel's potential vorticity is defined as $\Pi = (f + \nabla \times U) \cdot \nabla(z - \eta)$ (e.g., Kunze and Sanford 1993), where f is the Coriolis frequency, U the velocity vector, z the vertical coordinate, and η the vertical displacement of the isopycnal. Ertel's potential vorticity includes planetary vorticity, relative vorticity, linear vortex stretching, and nonlinear vorticity stretching, tilting, and twisting.

Based on the linear normal mode decomposition of small-scale oceanic motions, Lien and Müller (1992) proposed a theoretical scheme for separating linear internal waves and linear vortical motions (termed the vortical mode) using fields of the vertical component of relative vorticity (RV = $\partial_x v - \partial_y v$), horizontal divergence (HD = $\partial_x u + \partial_y v$), and vortex stretching (VS = $f\, \partial_z \eta$), where u, and v are horizontal velocity. To its linear limit, Ertel's potential vorticity reduces to PV = RV – VS. The linear vortical mode (vm) represents geostrophic motion and carries the linear potential vorticity. Linear internal waves (iw) carry no potential vorticity.

Kinematic properties of the vortical mode and linear internal waves can be summarized by their polarization relations expressed as

$$HD_{vm} = 0 \tag{1}$$

$$RV_{vm} = -B^2 VS_{vm} \tag{2}$$

$$\partial_t RV_{iw} = -f\, HD_{iw} \tag{3}$$

$$RV_{iw} = VS_{iw} \tag{4}$$

where the Burger number $B = \frac{N\alpha}{f\beta}$, N is the buoyancy frequency, α the horizontal wavenumber magnitude, and β the vertical wavenumber magnitude. The opposite signs between RV_{vm} and VS_{vm} can be derived by the thermal wind relation.

Kinetic energy and potential energy can be decomposed to linear internal wave and the linear vortical mode components as

$$E_{vm} = \frac{1}{2} N^2 PV^2 / [f^2 (1 + B^2) \beta^2] \tag{5}$$

$$KE_{vm} = B^2 PE_{vm} \tag{6}$$

$$E_{iw} = E_{total} - E_{vm} \tag{7}$$

$$KE_{iw} = PE_{iw} \frac{(N^2 - \omega^2)}{N^2} \frac{(\omega^2 + f^2)}{(\omega^2 - f^2)} \tag{8}$$

where *KE* and *PE* represents kinetic energy and potential energy, and $E = KE+PE$. E_{vm} and E_{iw} are the energy of the vortical mode and linear internal waves, respectively, and $E_{total} = E_{vm} + E_{iw}$.

Decomposition into vortical mode and internal wave components using EM-APEX float observations

Spectra of RV and HD and their coherence and phase spectra are computed using observations taken during setting 1, and averaged over the depth range between 70 and 150-m depth (Fig. 3). RV and HD are coherent with a 90° phase difference. Similarly, RV and VS are coherent and in-phase in the internal wave frequency band (Fig. 4). These two results imply that processes in the internal wave frequency band follow closely the polarization relations for linear internal waves, expressed in eqs. (3) and (4). That is, the vortical mode is much weaker than internal waves in the internal wave frequency band.

Observed fluctuations of RV and VS at setting 1 are decomposed into the vortical mode and internal wave components as proposed by Lien and Müller (1992) (Figs. 5 and 6). Vertical wavenumber and frequency spectra of vortical mode and internal wave components are computed following eqs. (5) and (7). The internal wave energy is stronger than vortical mode energy in the entire observed wavenumber range (Fig 7). The vortical mode is stronger than internal waves at frequencies smaller than f. Internal waves are stronger than the vortical mode in most of the internal wave frequency band (Fig. 8), further supporting results in Figs. 3 and 4. In computing the vortical mode energy, Burger number B is computed using the ratio of RV_{vm} and VS_{vm}, following eq. (2). Burger number of the vortical mode is O(1).

Turbulence observations from EM-APEX floats

The χ sensor provided high-quality observations of temperature variance. This was used to compute χ, which leads to KE dissipation rate ε and vertical diffusivity K_v. Vertical profiles of turbulence properties averaged over three settings are shown in Fig. 9.

Primary conclusions of the experiment are

- EM-APEX float array is a powerful tool in assessing the motion and water properties on small scales: 21 floats, simultaneous profiles
- For setting 1, there is a distinct background internal wave field, shown in the compensation of relative vorticity and vortex stretching
- Anomalous potential vorticity is present in setting 1 with magnitudes around $0.1 f$, which could be due to advection of PV across the field but still needs resolution
- For setting 2, there is a movement through a salinity front, which shows high anomalous PV values on the order of $0.5 f$. For the period, thermal wind balance is maintained across the front.

Some primary scientific conclusions are

- Background internal wave energy in the continuum varies from 0.5 GM at settings 1 and 2 to ~0.9 GM at setting 3
- RV, VS, and energy decompose into VM and IW (a first successful decomposition)

- $E_{VM} \sim 1/14\ E_{total}$, $V_{VM} \sim 1.2$ cm s^{-1} , and $PV_{VM} \sim 0.1\ f$
- At 20–40 m vertical wavelengths, $E_{VM} = E_{IW}$
- χ-EM-APEX floats captured the major portion of the temperature gradient spectrum and provide quality estimates of χ, K_v, and ε
- $K_v = 5 \times 10^{-6}$ m^2 s^{-1} at the level of the injected dye
- K_v decreases by more than 3 decades in the upper 40 m, implying the potential strong interplay between vertical diffusion and isopycnal diffusion and dispersion
- Turbulence is the weakest at setting 1, strong at setting 3 in the upper 40 m, and strong at setting 2 below 40 m.

IMPACT/APPLICATION

The operation of a swarm of autonomous vehicles simultaneously profiling is a breakthrough advance in the measurement of submesoscale ocean variability. The simultaneity of spatially separated observations eliminated the contamination caused by time differences between sequential observations, the classic scourge of field oceanography. That is, observations at a single site consist of fluctuations caused by both time and space dependencies. Thus, the difference between two observations separated both in time and space contains contributions from both variables. The ability to separate temporal and spatial gradients is a large step forward. Our use of a swarm of AUVs, all programmed to operate in unison, has now demonstrated the advantages over the more traditional methods. During this field study, over 8,000 CTD and velocity profiles were obtained in three experiments.

TRANSITIONS

The EM-APEX float resulted from a SBIR contract from ONR to Webb Research. This instrument has already begun to have an impact on a variety of experiments. The recent ONR DRI projects that the PI has been involved in have EM-APEX components. Other investigators have purchased and used these floats, such as James Girton, Eric Kunze, Mike Gregg, Helen Phillips (U. Tasmania), Jody Klymak (U. Victoria), and Indian oceanographers. NAVO is reported to be considering purchasing some.

RELATED PROJECTS

Studies of the Origins of the Kuroshio and Mindanao Currents with EM-APEX Floats and HPIES (N00014-10-1-0468). This is a component of the Origins of the Kuroshio and Mindanao Currents DRI. We deployed 5 HPIES (Horizontal electric field, pressure and IES) surrounding a moored array NE of Luzon Island. The purpose of the HPIES is to determine barotropic velocity from the electric field and baroclinic velocity from PIES in a triangle around a mooring. In addition, EM-APEX floats were deployed in the NEC as it approaches the Philippine Island and bifurcates into the Kuroshio Current going northward and Mindanao Current flowing southward.

REFERENCES

Kunze, E., and T. B. Sanford (1993). Submesoscale dynamics near a seamount. Part I: Measurements of Ertel vorticity, *J. Phys. Oceanogr.*, **23**, 2567-2588.

Kunze, E., J. M. Klymak, R.-C. Lien, R. Ferrari, C. M. Lee, M. A. Sundermeyer, and L. Goodman. (2015). Submesoscale water-mass spectra in the Sargasso Sea, *J. Phys. Oceanogr*., **45**, 1325-1338.

Lien, R.-C. and P. Müller (1992). Normal mode decomposition of small-scale oceanic motions, *J. Phys. Oceanogr.,* **22**, 1583-1595.

Müller, P., (1984). Small-scale vortical motions, *Internal Gravity Waves and Small-Scale Turbulence*, Proceedings, Hawaiian Winter Workshop, P. Müller, R. Pujalet, 249–262, *Hawaii Institute of Geophysics,* Honolulu.

Okubo, A., and C. C. Ebbesmeyer (1976). Determination of vorticity, divergence, and deformation rates from analysis of drogue observations, *Deep-Sea Res.*, **23**, 349-352.

PUBLICATIONS (wholly or in part supported by this grant)

Shcherbina, Y. A. et al. (2015). The LatMix summer campaign: Submesoscale stirring in the upper ocean, *Bull. Amer. Meteorol. Soc.* [in press, refereed]

Kunze, E., J. M. Klymak, R.-C. Lien. R. Ferrari, C. M. Lee, M. A. Sundermeyer, and L. Goodman. (2015). Submesoscale water-mass spectra in the Sargasso Sea, *J. Phys. Oceanogr*., **45**, 1325-1338. [published, refereed]

Sanford, T.B. (2013). Spatial structure of the thermocline and abyssal internal waves, *Deep-Sea Res. Part II.* **85,** 195-209. [published, refereed]

Szuts, Z.B., and T. B. Sanford (2013). Observations of vertically-averaged velocity in the North Atlantic Current, *Deep-Sea Res. Part II.* **85**, 210-219. [published, refereed]

Terker, S.R., T. B. Sanford, J. H. Dunlap, and J. B. Girton (2013). EM-POGO: A simple, absolute velocity profiler, *Deep-Sea Res. Part II.* **85,** 220-227. [published, refereed]

Mrvalijevic, R. A., P. G. Black, L. R. Centurioni, E. A. D'Asaro, S. R. Jayne, C. Lee, R.-C. Lien, J. Morzel, P. P. Niiler, L. Rainville, T. B. Sanford, and T.-Y. Tang (2013). Evolution of the cold wake of Typhoon Fanapi, *Geophys. Res. Lett.* **49**, 316-321. [published, refereed]

Lien, R.-C., T.B. Sanford, S. Jan, M.-H Chang, and B.-B. Ma (2013). Internal tides on the East China Sea Continental Slope, *J. Mar. Res.*, **71**, 151-185. [published, refereed]

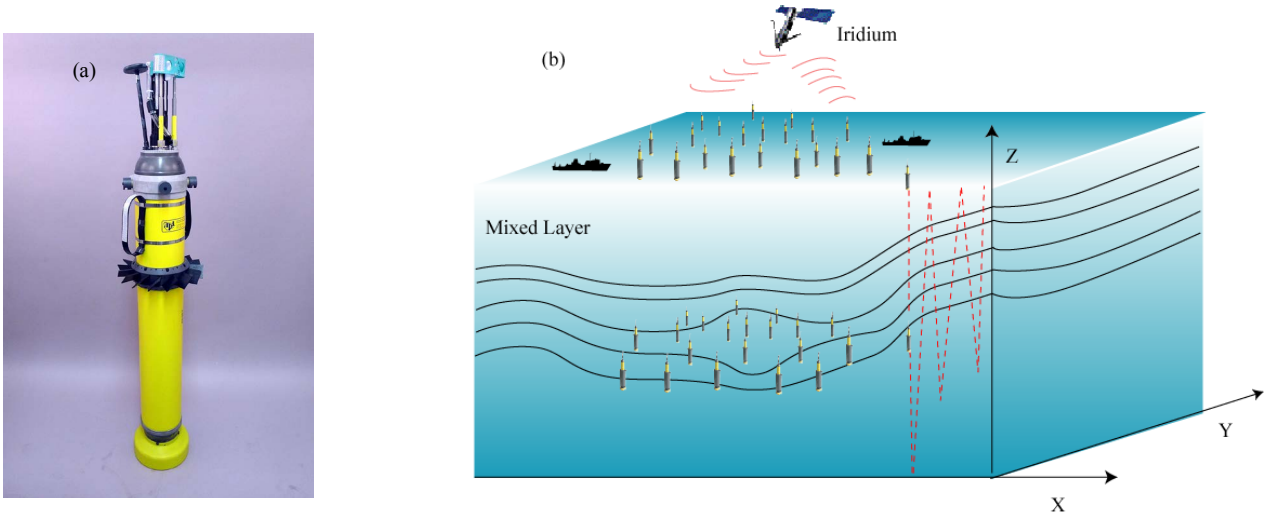

Fig. 1: (a) EM-APEX float with dual χ sensors. (b) Schematic of a spatial array of 10 microstructure EM-APEX floats (χ-EM-APEX floats) and 10 regular EM-APEX floats. N.B. The χ sensors were mounted so as to be out of the wake produced by the Iridium antenna, which will be tilted to the side in the so-called "Mai Tai" mounting.

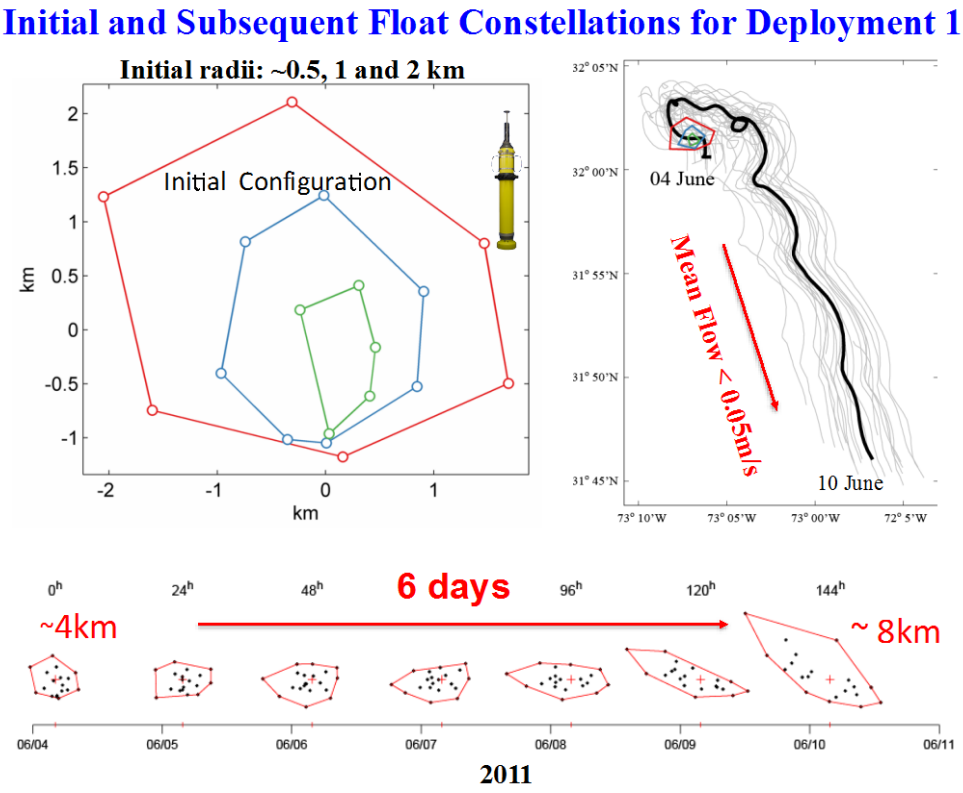

Fig. 2: Upper left panel: Initial configuration of EM-APEX floats. Upper right panel: Movement of the array during experiment with array center in bold line and individual floats in thin gray lines. Bottom panel: Relative motion of floats over 6 days.

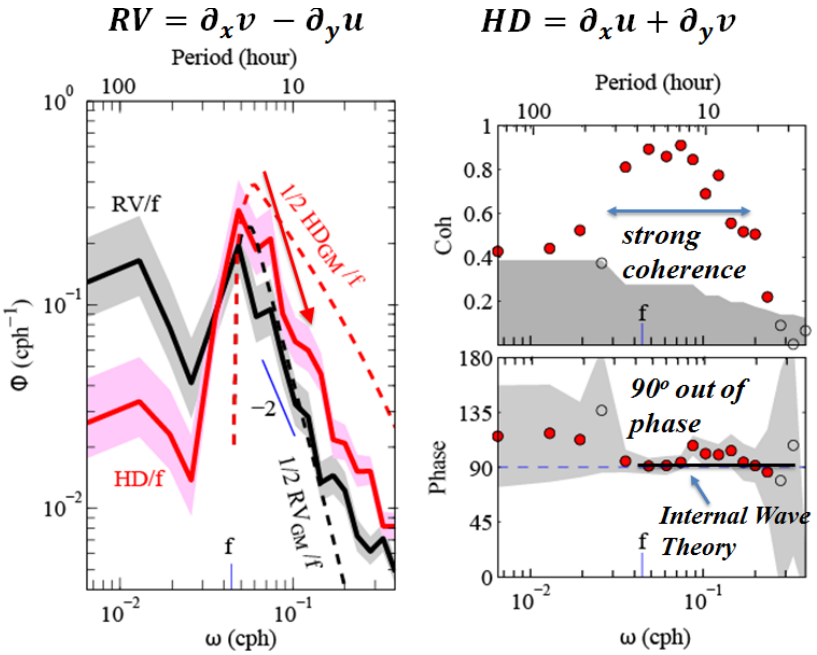

Fig. 3: Left panel: Power spectra of RV (black curve) and HD (red curve) normalized by f. Right panels: Coherence and phase spectra between RV and HD. Black and red dashed curves in left panel represent one half of normalized RV and HD spectra of GM model, respectively. Red dots in right panels highlight significant coherence. Note highest correlation of RV and HD near 90° phase, especially in the internal wave frequency band, as expected for internal waves.

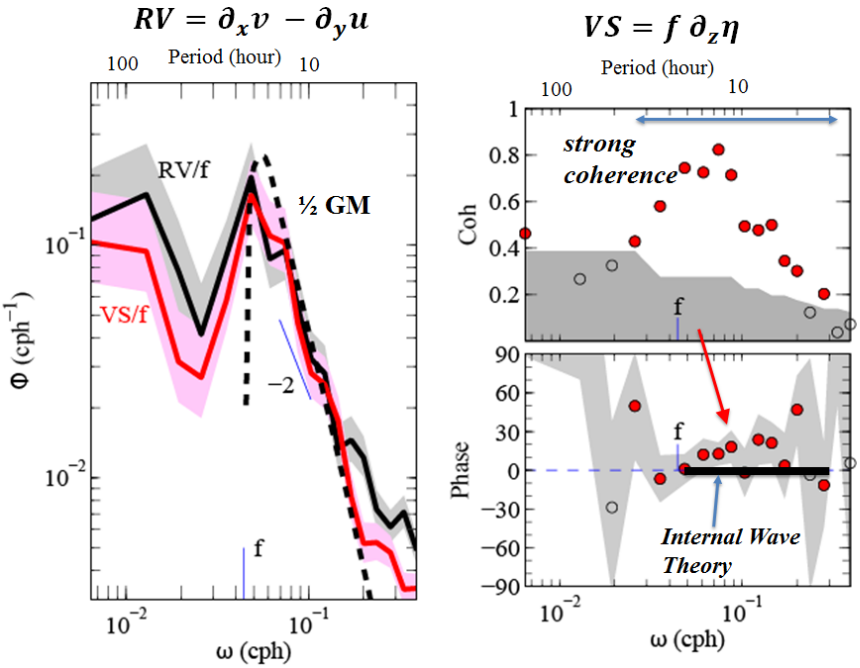

Fig. 4: Left panel: Power spectra of RV (black curve) and VS (red curve) normalized by f. Right panels: Coherence and phase spectra between RV and VS. Black and red dashed curves in left panel represent one half of normalized RV and VS spectra of GM model, respectively. Red dots in right panels highlight significant coherence. Note highest correlation of RV and VS near 0° phase, especially in the internal wave frequency band, as expected for internal waves.

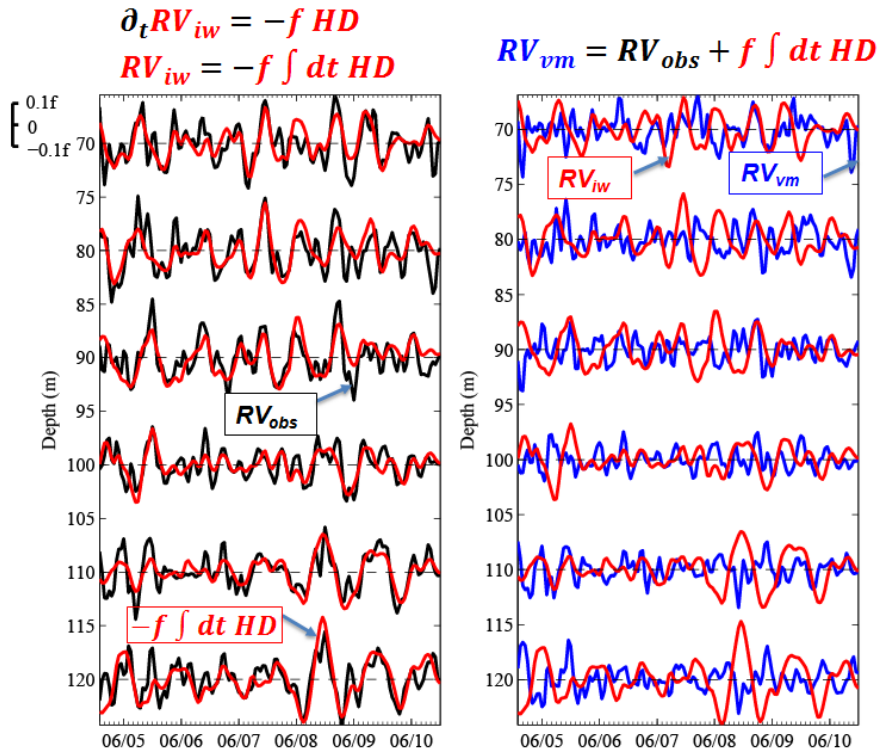

Fig. 5: Decomposition of observed RV (black curves) into the vortical mode (blue curves) and internal wave (red curves) components at different depths.

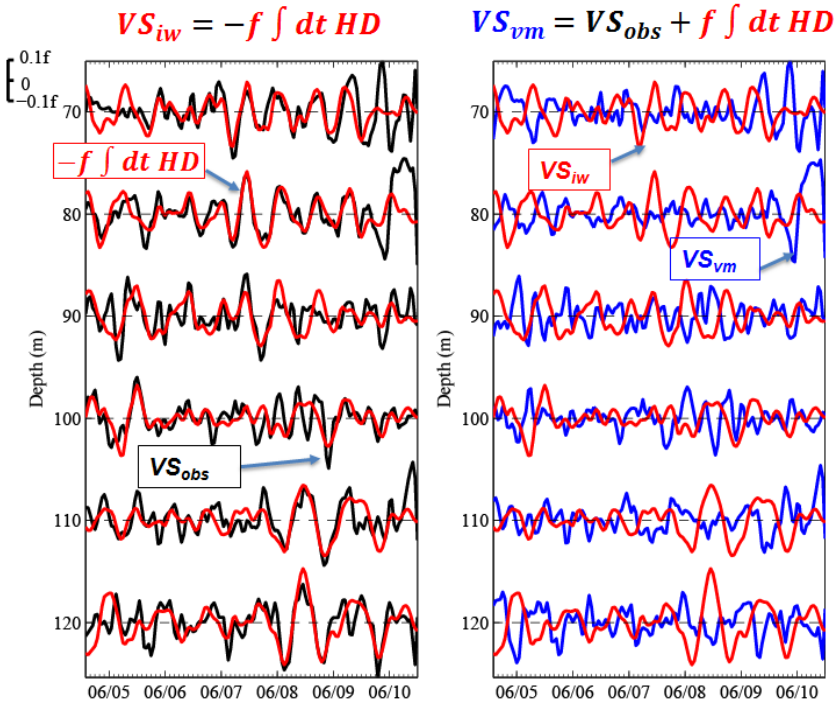

Fig. 6 Decomposition of observed VS (black curves) into the vortical mode (blue curves) and internal wave (red curves) components at different depths.

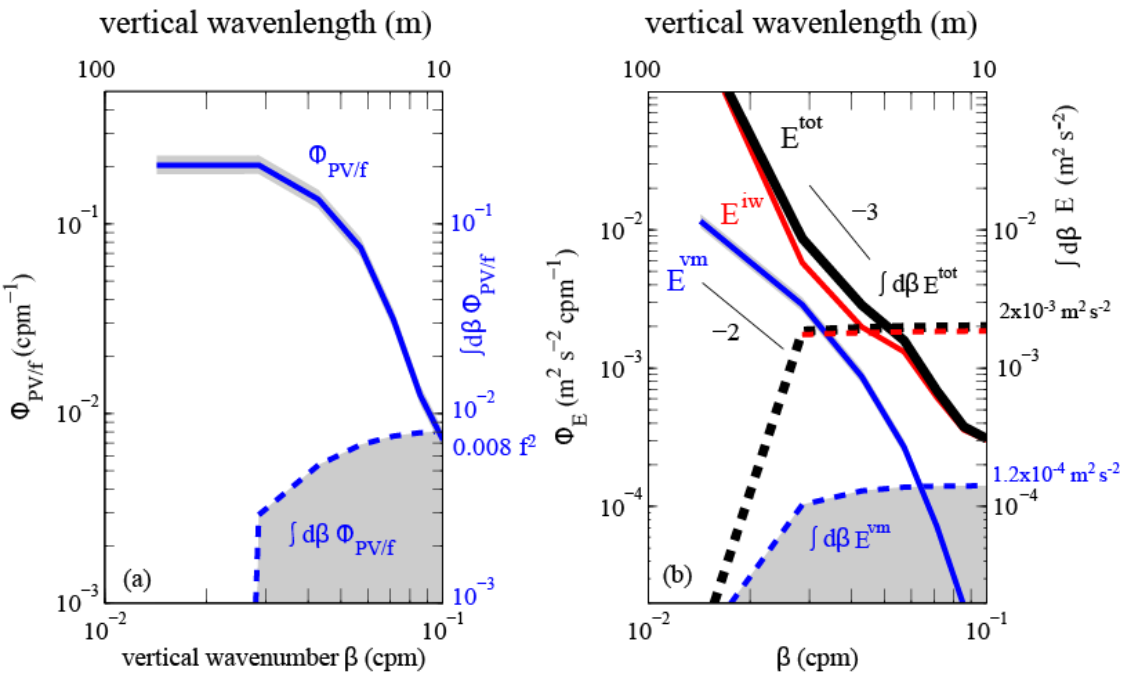

Fig. 7: Vertical wavenumber spectra of PV and total energy. (a) Vertical wavenumber spectrum of PV normalized by f. (b) Spectra of total (black curve), internal wave (red curve) and vortical mode spectra (blue curve). Total energy variance is about 10 times the VM variance. The rms VM velocity is 1.2 cm s^{-1}. Blue dashed curves in (a) represents the accumulated enstrophy. Blue, red, and black dashed curves in (b) represent the accumulated total energy of the vortical mode, the internal wave, and the total field, respectively.

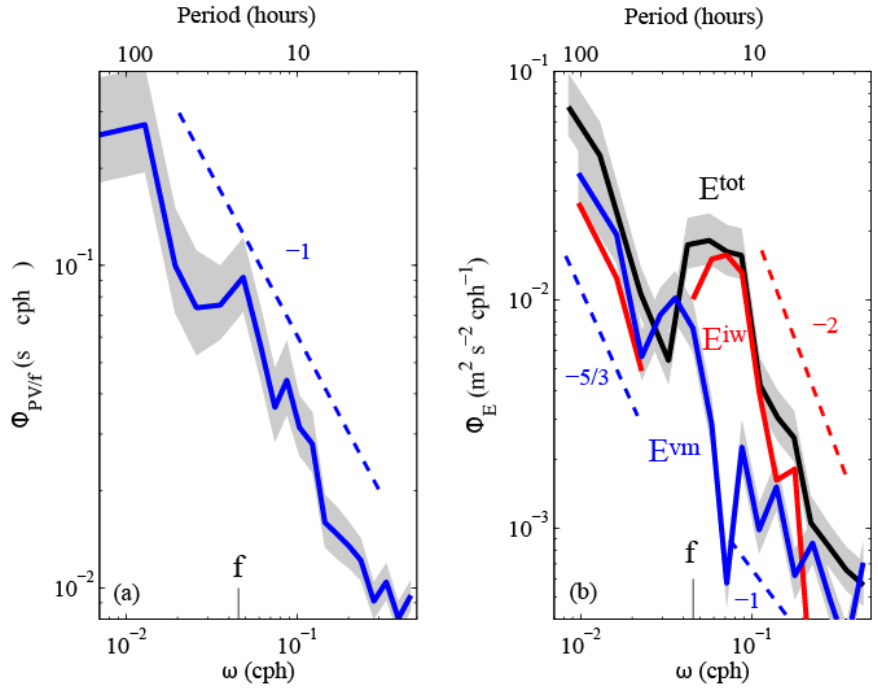

Fig. 8: Frequency spectra of PV and total energy. (a) PV/f spectrum. (b) Energy spectra for observations (red curve) and VM (blue curve). Dashed lines illustrate various spectral slopes for reference.

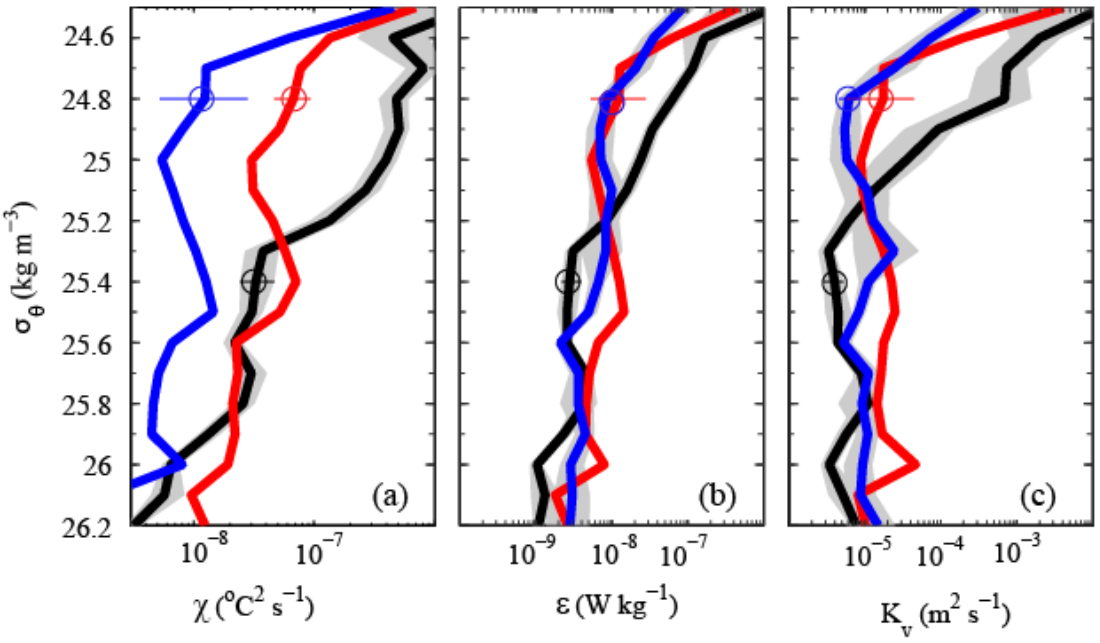

Fig. 9: Vertical profiles of χ, ε and K_v from the χ sensors averaged over settings 1 (black curves), 2 (red curves), and 3 (blue curves). Circles indicate depths where dye was injected.